




Article

Load Transfer during Magnetic Mucoperiosteal Distraction in Newborns with Complete Unilateral and Bilateral Orofacial Clefts: A Three-Dimensional Finite Element Analysis

Prasad Nalabothu ^{1,2,*} , Carlalberta Verna ¹, Benito K. Benitez ² , Michel Dalstra ^{1,†} and Andreas A. Mueller ^{2,†} 

¹ Department of Paediatric Oral Health and Orthodontics, University Center for Dental Medicine UZB, 4058 Basel, Switzerland; carlalberta.verna@unibas.ch (C.V.); michel.dalstra@unibas.ch (M.D.)

² Department of Oral and Craniomaxillofacial Surgery, University Hospital Basel, 4031 Basel, Switzerland; benito.benitez@usb.ch (B.K.B.); andreas.mueller@usb.ch (A.A.M.)

* Correspondence: prasad.nalabothu@unibas.ch; Tel.: +41-61-328-60-95

† Joint last authors.

Received: 17 September 2020; Accepted: 23 October 2020; Published: 31 October 2020



Abstract: The primary correction of congenital complete unilateral cleft lip and palate (UCLP) and bilateral cleft lip and palate (BCLP) is challenging due to inherent lack of palatal tissue and small extent of the palatal shelves at birth. The tissue deficiency affects the nasal mucosa, maxillary bone and palatal mucosa. This condition has driven the evolution of several surgical and non-surgical techniques for mitigating the inherent problem of anatomical deficits. These techniques share the common principle of altering the neighboring tissues around the defect area in order to form a functional seal between the oral and nasal cavity. However, there is currently no option for rectifying the tissue deficiency itself. Investigations have repeatedly shown that despite the structural tissue deficiency of the cleft, craniofacial growth proceeds normal if the clefts remain untreated, but the cleft remains wide. Conversely, craniofacial growth is reduced after surgical repair and the related alteration of the tissues. Therefore, numerous attempts have been made to change the surgical technique and timing so as to reduce the effects of surgical repairs on craniofacial growth, but they have been only minimally effective so far. We have determined whether the intrinsic structural soft and hard tissue deficiency can be ameliorated before surgical repair using the principles of periosteal distraction by means of magnetic traction. Two three-dimensional maxillary finite element models, with cleft patterns of UCLP and BCLP, respectively, were created from computed tomography slice data using dedicated image analysis software. A virtual dental magnet was positioned on either side of the cleft at the mucoperiosteal borders, and an incremental magnetic attraction force of up to 5 N was applied to simulate periosteal distraction. The stresses and strains in the periosteal tissue induced by the magnet were calculated using finite element analysis. For a 1 N attraction force the maximum strains did not exceed 1500 μ strain suggesting that adaptive remodeling will not take place for attraction forces lower than 1 N. At 5 N the regions subject to remodeling differed between the UCLP and BCLP models. Stresses and strains at the periosteum of the palatal shelf ridges in the absence of compressive forces at the alveolar borders were greater in the UCLP model than the BCLP model. The findings suggest that in newborns with UCLP and BCLP, periosteal distraction by means of a magnetic 5 N attraction force can promote the generation of soft and hard tissues along the cleft edges and rectify the tissue deficiency associated with the malformation.

Keywords: cleft lip and palate; finite element model; periosteal bone remodeling; unilateral cleft palate; bilateral cleft palate; distraction

1. Introduction

Cleft lip and palate (CLP) is the most common craniofacial malformation, affecting one in every 500 to 700 live births, thus accounting for about 220,000 new cases each year worldwide with disparity across geographic areas, racial groups, and socioeconomic status [1]. No effective preventive measures exist. The ongoing manifestation of CLP as well as its broad implications on psychological well-being, speech, orofacial development, and therapeutic burden underline the need to identify and targeting the intrinsic causes [2–4].

The etiology of CLP is complex, which could occur as a result of multiple genetic and environmental factors or a combination of both [5,6]. The clefting of the lip and/or palate may occur in a unilateral or bilateral fashion, and the embryological pattern of clefting results from a fusion failure during the development of maxilla and palate. The normal fusion of the medial frontonasal process with the maxillary process of the first pharyngeal arch takes place at 4–6 weeks of gestation forming a primary palate [7]. A complete fusion failure results in a cleft of the lip through the vermillion border that extends to the nasal sill and in a cleft of the alveolar process [7]. The cleft of the secondary palate occurs at 8–12 weeks of gestation due to fusion failure of the palatal shelves of the maxillary processes [8,9] that results in a cleft in the palatal roof and soft palate that extends to the uvula.

Affected children have a range of both functional and esthetic problems. They comprise feeding difficulties at birth due to incomplete oral seal, swallowing, nasal regurgitation, respiratory problems, hearing difficulties due to abnormalities in the palatal musculature, and speech impairments due to air escape and articulation problems [10]. Therefore, an ideal early and complete cleft treatment would allow the normalizing of food intake, speech development, growth and esthetics - while imposing minimal treatment burden to child and family.

Several different surgical protocols have been advocated for managing children with CLP. The amount of palatal mucosa present and timing of the surgery play important roles in healing success after surgery. Clefting of the palate at birth structurally results in 16% less palatal mucosa compared with a normal child [11] and anatomically smaller palatal shelves on the cleft and noncleft sides [12,13]. The intrinsic tissue deficiency in the palate has no spontaneous improvement trend. It persists until adulthood in both unilateral cleft lip and palate (UCLP) and bilateral cleft lip and palate (BCLP) [14].

A scientific basis was proposed in 2005 for determining the optimal conditions for palatal cleft closure in complete UCLP and BCLP [15]. This should be performed when the surface area of the cleft space does not exceed 10% of the surrounding palatal surface bounded by the alveolar ridges, because under these circumstances the facial growth is less affected, independent of the patient's age at surgery [15]. This recommendation may be applicable for clefts which are smaller in size, whereas in cases of wider clefts it is imperative for surgeons to mobilize the tissue adjoining the cleft more extensively which may lead to open wound areas that undergo secondary healing. This may lead to structural tissue deficiencies and pronounced interference with the normal growth and development of the midface [16].

The use of a palatal appliance for presurgical maxillary orthopedics is a widely accepted non-surgical therapeutic adjunct for addressing the problem of tissue deficiency in wider clefts. Such an appliance approximates the palatal shelves and thus reduces the alveolar and palatal cleft width prior to surgery [17]. The effect of those appliances on the growth is controversial. Some proponents of this technique have claimed that gradual adaptations of the appliance can stimulate palatal tissue growth [18,19]. Others have shown that this approach resulted in retarded growth of the palatal tissue [20]. Finally, a randomized controlled trial concluded that using a palatal appliance does not result in any permanent growth change or tissue gain [21].

Various surgical techniques have also been applied in an attempt to mitigate the problems of tissue deficiency. These techniques varied between surgeons, and there is still no consensus on which is the best protocol for treating CLP patients. Seventeen different surgical sequences for repairing unilateral complete clefts were identified in a survey of over 201 European cleft centers [22].

Three main surgical principles to mitigate the tissue deficiency in CLP have evolved [23]. The first principle limits the closure only to either the oral or the nasal mucosa layer by applying a so called single-layer closure [24–27]. This procedure involves turning over the mucosa from either the oral or the nasal cavity like a book page while leaving an open wound on the back side of the turned-over mucosa. The second principle involves detaching the oral tissue and shifting it over the cleft area while creating an open wound that heals outside the cleft area from where the tissue has been detached [28–30]. In the third principle, tissue from outside the palatal area is used to cover the open wound areas that result from the first or second technique [31–34]. While all of these surgical techniques are able to close the cleft gap using the available tissue, none of them result in the generation of new mucoperiosteal tissue.

Adjuvant therapies or strategies such as tissue expansion [35] and distraction osteogenesis (DO) [36] have been attempted to increase the volume of tissue in the areas of tissue deficiency in clefts. The principles of DO require a bone cut through the palatal shelf ridges. However, in infants this would damage the dental follicles that are embedded in the palatal shelf ridges. Most tissue engineering studies have focused on the application of biomaterials purely for bone generation [37]. However, the palatal cleft comprises bone and two mucosal layers, which makes it a difficult target for biomaterial or tissue-engineering techniques.

Animal experiments suggest that periosteal distraction osteogenesis (PDO) is an appealing option for utilizing the principles of DO [38–40] for combined bone and soft tissue generation without the need for a bone cut. PDO is performed by gradual lift-up on the mucoperiosteum from the underlying bone by applying mechanical loading. The physical tissue strain and biological tissue stimulus to bone and periosteum lead to new tissue formation. We therefore address PDO as a potential treatment strategy to target the tissue deficiency in orofacial clefts while using magnetic forces to exert the necessary tissue strain. Magnetic forces have been used in orthodontics to generate tooth movement and to promote tissue reactions [41].

Finite element (FE) analysis is a numerical tool to compute the stress and strain fields in the bone structure under external loading. It thereby reveals the distribution of the internal loads and deformations. Computational FE analysis has provided crucial basic data for understanding mechanical interactions between the magnets and mucoperiosteal tissue for tissue expansion [42]. The loading distribution depends on the shape and size of individual anatomical structures and malformation. Previously, this method has been used to assess the maxillary load transfer during conventional DO in patients with cleft lip and palate [43].

In our previous study we have examined the feasibility of dental magnets as distraction devices in newborns with UCLP [44]. Unilateral clefts form 76% of all CLP cases worldwide which still leaves the BCLP, accounting for one fourth (24%) of all CLP unaddressed [45]. As the anatomy of BCLP is different from UCLP, it is the aim of this study to compare the load transfer of magnetic forces used for PDO in both UCLP and BCLP in *silico* models. It examines whether the forces reach the threshold necessary for regeneration of the hard and soft tissue volumes along the cleft edges in both UCLP and BCLP.

2. Materials and Methods

2.1. Ethical Statement and Patient Data

The reported investigations and procedures were conducted according to the principles expressed in the Declaration of Helsinki. Two computed tomography (CT) scans of anonymized 2- and 3-week-old newborns with complete UCLP and BCLP, respectively, were obtained from an existing database and analyzed. The DICOM data sets of 2 CT scans were obtained from a commercial CT scanner using a voxel size of 0.3 mm (Philips CT scanner, Eindhoven, The Netherlands).

2.2. Model Construction

The CT scans of the UCLP and BCLP newborns were imported into dedicated image analysis software (Mimics version 19, Materialise, Leuven, Belgium) and three-dimensional (3D) surface models were generated by thresholding and selecting only the hard tissues of the cranium and maxilla. The region of interest was further defined by virtually removing all structures except for the midface, including the maxilla and the adjoining bony segments of the face (first, second and third rows in Figure 1).

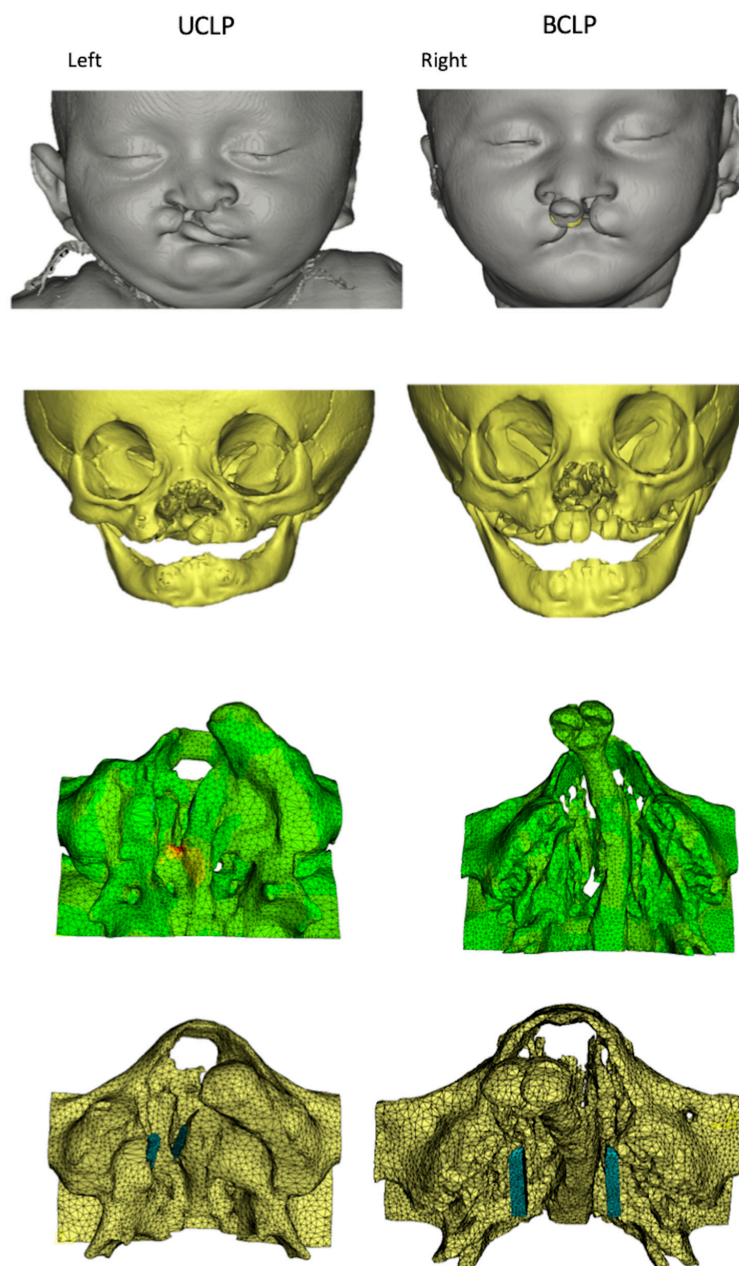


Figure 1. From computed tomography scans to finite element (FE) models with magnets in the unilateral cleft lip and palate (UCLP, left column) and bilateral cleft lip and palate (BCLP, right column). Frontal views of three-dimensional reconstructions of the soft tissue (first row) and hard tissue (second row). Regions of interest of the FE models (third row) and the models with magnetic strips which are blue in color (fourth row).

2.3. Magnet Implantation

The rare-earth permanent magnets used for in vitro testing were constructed from a neodymium-boron-iron alloy (Dyna WR magnets, Dyna Dental Engineering, Halsteren, The Netherlands). The magnets were disc shaped with a height of 1.7 mm and a diameter of 4.5 mm (02MS1 Dyna WR magnet S3). The mucoperiosteum borders on the cleft and non-cleft sides were covered with two 23 mm long parallel bars of five magnets each placed in a row in the UCLP and BCLP models (Figure 1, fourth row). In the following analyses, each row of the magnets was assumed to exert attracting forces relative to the oppositely placed row of magnets. Experimental force-distance curves for these magnets were measured [44] with the results used to define incremental forces with a magnitude of up to 5 N to either side of the cleft in the UCLP and BCLP models.

2.4. FE Model Design

The FE mesh was constructed based on the CT scans of the 3D UCLP and BCLP models. The UCLP FE mesh consisted of 238243 4-node tetrahedral elements with 43822 nodes, whereas the BCLP FE mesh consisted of 409027 4-node tetrahedral elements with 74551 nodes. The position of the centroid of each element was calculated and a gray scale was associated with it based on spatial interpolation of the gray scale values of the nearest voxels. The gray scale values from the CT scans were correlated with the material density and the material stiffness. Relevant material properties were assigned for the elements representing bone, arithmetic relationships between gray scale values, apparent densities and Young's moduli [46–49]. Depending on its apparent density and the associated gray scale values, the bone tissue was stratified into ten different material property groups, ranging from very low-density cancellous bone (bone 1) to dense cortical bone (bone 10). The material properties of these ten types of bone (apparent density, Young's modulus, Poisson's ratio and yield strength) were same as used by Nalabothu et al. [44]. To highlight the compositional difference between the UCLP and BCLP model each type of bone density (bone 1 to bone 10) has been cumulatively compared between both models (Figure 2).

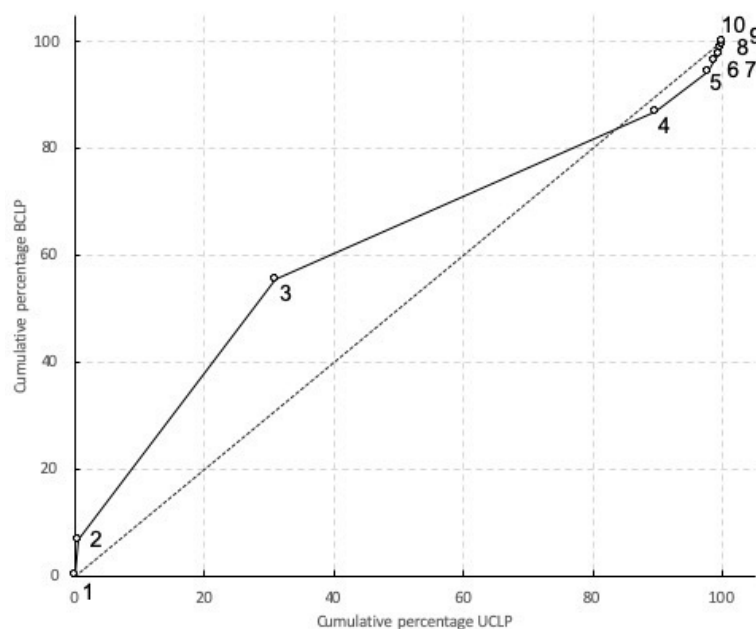


Figure 2. The cumulative percentage of the ten material property groups for the unilateral cleft lip and palate (UCLP) and bilateral cleft lip and palate (BCLP) models, respectively. The material properties of the ten different bone types are retrieved from Nalabothu et al. [44].

2.5. FE Analysis

The UCLP and BCLP FE models were exported from the image analysis program in NASTRAN format and imported into an FE analysis program (Strand7, Sydney, Australia). The material properties of the bone were assumed to be non-linear, with its stress-strain curves in the ten groups adapted so that the bone would behave as a perfectly plastic material whose compressive strength was 150% higher than its tensile strength [50]. The FE analyses were conducted using a nonlinear solver with logarithmically increasing increments from 0.01 to 1 (100% load). The calculated stresses and the associated strains were used for post-processing.

3. Results

The application of a 1 N attraction force did not produce strain levels in the 1500 μ strain range in both the UCLP and BCLP model. As this was considered a minimum requirement for adaptive remodeling, in the following only the results for a 5 N attraction force are presented.

3.1. Overall Deformation of the Maxilla

The maximum deformation in the UCLP and BCLP models occurred around the sites adjacent to the magnetic strips at the vomer edge of the greater and lesser segments of the palatal shelf ridge. The overall deformation was greater in the UCLP model (left column of Figure 3) than in the BCLP model. In the BCLP model, the deformations occurred more in the posterior area of the palatal shelf ridges (right column of Figure 3) than in the anterior one.

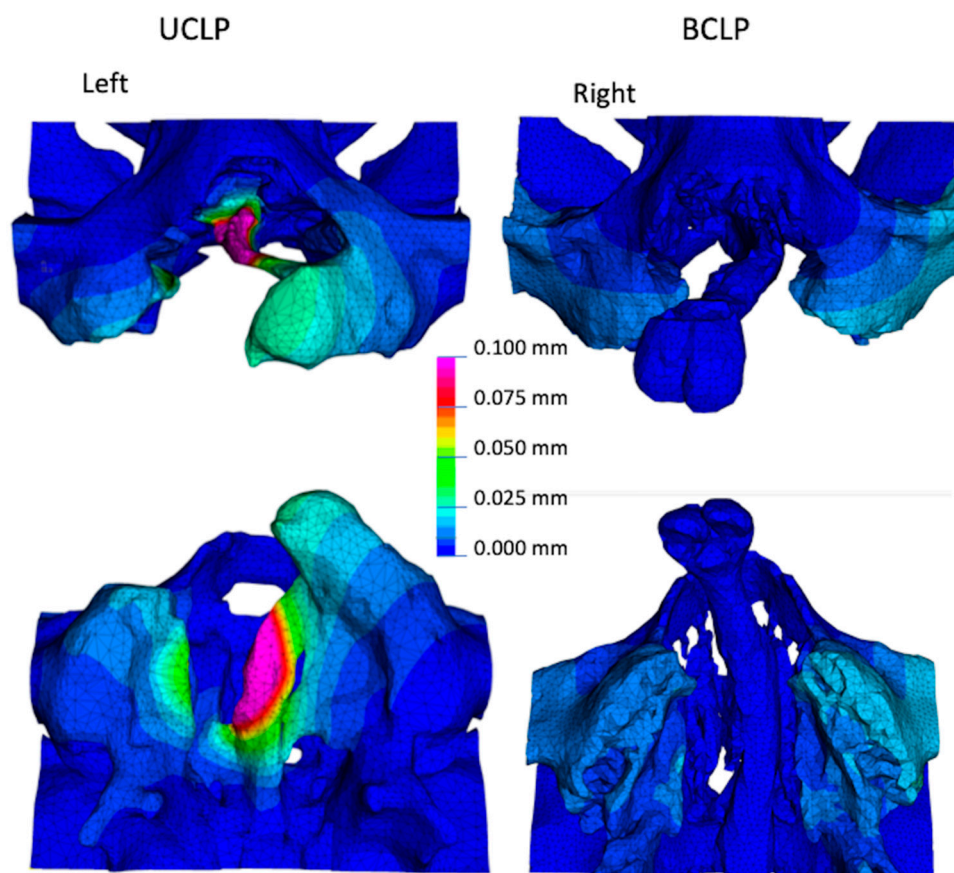


Figure 3. Distribution of the overall periosteal deformation in mm for 5 N loading in the UCLP (left column) and BCLP (right column) models. Frontal (top row) and palatal (bottom row) views are shown.

3.2. Stresses and Strains in the Maxilla

The obtained stress/strain components of the UCLP and BCLP FE models in the X-direction (coronal), Y-direction (medial/lateral) and Z-direction (anterior/posterior) were different in each aspect. In the BCLP model no strains higher than 1500 μ strain were seen for a magnetic load of 1 N (Figure 4). However, a load of 5 N regions with strains beyond 1500 μ strain were observed though less than the UCLP model [44].

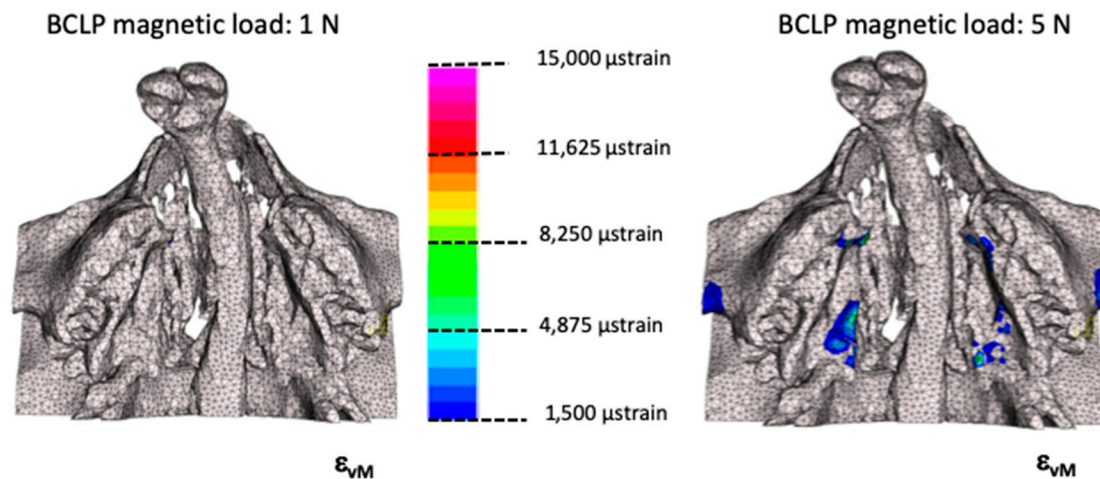


Figure 4. Areas showing the overall strain levels in BCLP model during loading of 1 N (left) and 5 N (right) from the palatal view.

The orthogonal stresses in the coronal (X) direction occurred in the UCLP model mainly at the anterior part of the ridge of the lesser segment and the posterior part of the vomer edge (Figure 5: left column, top row), while in the BCLP model it occurred bilaterally in the posterior border of palatal shelf ridge (Figure 5: right column, top row). The orthogonal stresses in the medial/lateral (Y)-direction occurred in the UCLP model mainly at the middle portion of the lesser segment's ridge and in some sparse areas at the middle portion of the vomer edge and the greater segment's ridge (Figure 5: left column, second row), while in the BCLP model it occurred bilaterally on the palatal shelf ridges at the anterior tip and posterior border (Figure 5: right column, second row).

The orthogonal stresses in the antero/posterior (Z) direction occurred in the UCLP model mainly on the anterior portion of the lesser segment's ridge and on the middle portion of the vomer edge and on the anterior portion of the greater segment's ridge (Figure 5: left column, third row), while there were no stresses in this direction in the BCLP model (Figure 5: right column, third row).

The von Mises stresses (stress intensity) in the UCLP model were highest on the entire greater and lesser palatal shelf ridges and on the vomer edge (Figure 5: left column, bottom row), while in the BCLP model von Mises stresses were highest bilaterally on the anterior and posterior parts of the palatal shelf ridges. (Figure 5: right column, bottom row).

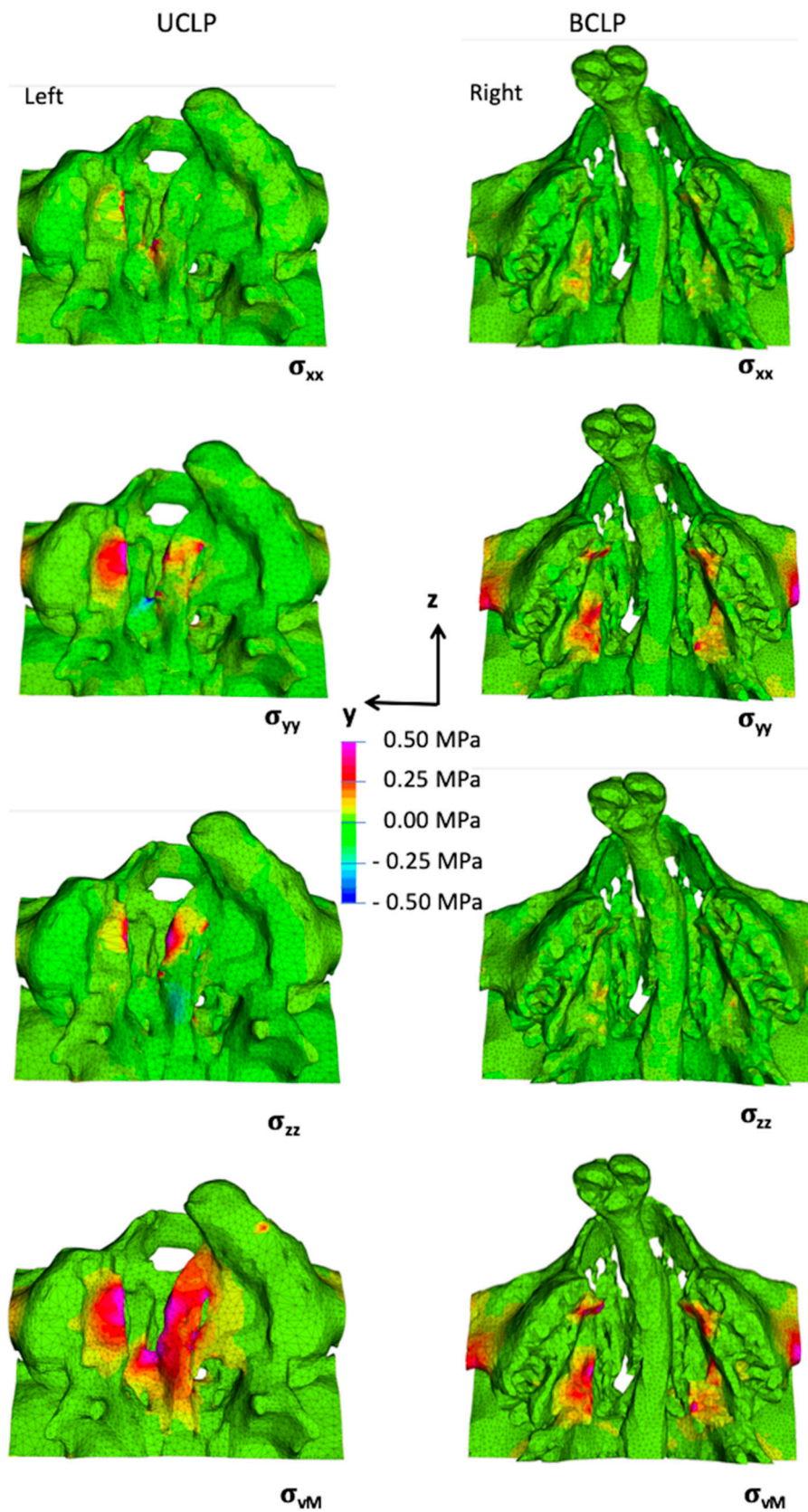


Figure 5. Distributions of the three orthogonal stress components and the von Mises stresses under a 5 N load from palatal view in the UCLP (left column) and BCLP (right column) models. The top second and third rows show the orthogonal stresses in the X-, Y-, and Z-directions, respectively, and the bottom row shows the von Mises stresses (stress intensity).

4. Discussion

The success of surgical hard palate closure in UCLP and BCLP is dependent on the availability of tissue in relation to the cleft area that needs to be closed. In wider clefts it is imperative to mobilize the tissue adjacent to the cleft more extensively, which leads to a wider tissue wound and tissue reparation rather than regeneration [51]. This situation may interfere with the normal growth and development of the midface and dentition [12,52]. The growth in patients with clefts remains a challenge regardless of which surgical protocol is applied. Applying adjuvant therapies before surgery can alleviate the problems of tissue deficiency to some extent by approximation of the palatal shelves using active presurgical orthopedics [53] or passive plate therapy [17], which facilitate tissue closure across the cleft area. However, the stocks of bone and soft tissue still remain deficient since such therapies do not aid in the regeneration of local tissue.

Therefore, in this study we tested a contrasting strategy based on increasing the bone and soft tissue prior to cleft surgical repair by means of magnetic periosteal distraction. It aims for true generation of the deficient osteo-mucoperiosteal tissue—thus, tackling the inherent palatal tissue deficiency which is a basic feature of the cleft malformation that does not disappear over time. With this intention, we analyzed the *in silico* stress distribution induced by magnetic strips placed on the cleft palatal shelves in newborns with UCLP and BCLP. We tested the hypothesis that magnets can generate bone inducing strains in UCLP and BCLP newborns.

Analyses of load transfer, by studying the distribution of stresses and strains, are a prerequisite before *in vivo* testing since incorrect loading or overloading may lead to disorganized tissue structures, eventually leading to tissue necrosis. Determining these stresses and strains *in vivo* is not feasible in newborns for ethical reasons, and so 3D *in silico* models were deemed a valid alternative approach. Although our experiments were confined to tissue generation by means of stresses induced by magnetic periosteal distraction, there is increasing evidence that magnetic fields can further promote bone regeneration directly by attracting growth factors, hormones and polypeptides to the implantation site [54]. The length of the magnetic strips was defined as 23 mm since the average length of hard palate at birth is 25.6 mm \pm 1.6 mm [55]. Previous tests on the magnetic attraction forces across porcine palatal mucosa (rugae) tissue allowed the simulation of the thickness of mucosa in the newborns [44].

In the present study we found that applying 5 N attraction forces using magnetic strips induced stresses in the UCLP and BCLP models mainly at the vomer edge and the palatal shelf ridges of the greater and lesser segments (left and right columns, Figure 3). Areas of tissue generation were delineated by applying the principles of Frost's Mechanostat theory, which states that mechanical loading influences the bone structure by changing the mass (amount of bone) and architecture (arrangement of surrounding tissues) if the induced strain exceeds 1500 μ strain. This implies that periosteal tissue regeneration will be induced at sites where the strain in the underlying bone exceeds 1500 μ strain, as the periosteum is mechanically subservient to the bone [56] (Figure 4).

The area of periosteal tissue that was subjected to at least 1500 μ strain was larger in the UCLP model than the BCLP model, which could be due to differences in material properties of the bone and anatomical variations. In the two FE models there is more low-density bone type 3 present in BCLP than in the UCLP model (Figure 2). Moreover, the direction of the magnetic forces is also more horizontally oriented in BCLP model compared to the UCLP model. The stresses and strains, able to induce adaptive remodeling, as exhibited in both UCLP and BCLP models, were localized to the area of the intrinsic tissue deficit of the cleft malformation while at the same time not affecting the neighboring areas, thus providing evidence that no compressive forces were transmitted to the alveolar ridges by the magnets.

The abovementioned geometrical and structural differences between the bone anatomy of the UCLP and BCLP mean that each will require a different design of implant. The larger cleft width in case of BCLP would make a more powerful magnet necessary to generate equivalent forces as in case of UCLP. Alternatively, the use of spacers to partially bridge the distance, or the placement of an auxiliary implant at the vomer could be considered as an option. The present findings obtained in

the UCLP and BCLP FE models might not be generalizable to all clefts of similar distances between the affected and non-affected segments, since the 3D bone morphology might vary even when the morphology in the cleft area is identical. However, the results of this study give guidance about the distribution of palatal load transfer around the cleft segments by inducing PDO within the optimal biological limits [56]. Future studies could test this hypothesis of mucoperiosteal distraction in an in vivo cleft animal model [57] in order to validate the findings of the present FE analyses.

5. Conclusions

The following conclusions can be drawn from this study

1. The present FE models have shown that the use of magnets as approved for dental applications can exert attraction with the potential to induce PDO around the greater and lesser segments of the palatal shelf ridge in cases of UCLP and BCLP.
2. A magnetic attraction force of 5 N was found to be sufficient to reach strain values in excess of 1500 μ strain in the palatal bone in both UCLP and BCLP models, and thereby have the potential to initiate adaptive remodeling.
3. The effects of magnetic load transfer were localized to their area of application, and did not spread out to distant structures.
4. The anatomical variations both in external bone geometry and internal bone composition affect the load transfer across the palate.

Author Contributions: Conceptualization, A.A.M. and C.V.; data curation, P.N. and M.D.; formal analysis, P.N. and M.D.; funding acquisition, C.V., A.A.M. and H.F.Z.; investigation, P.N. and M.D.; methodology, P.N., M.D. and A.A.M.; supervision, M.D., C.V. and A.A.M.; validation, P.N., A.A.M. and M.D.; visualization, P.N., A.A.M., B.K.B., M.D. and C.V.; writing—original draft, P.N.; writing—review and editing, P.N., M.D., B.K.B., C.V. and A.A.M. All authors have read and agreed with submitting this version of the manuscript.

Funding: This study was partially funded by a research grant from the Freiwillige Akademische Gesellschaft (FAG), Basel, Switzerland.

Acknowledgments: The authors thank Dyna Dental Engineering B.V., Halsteren, Netherlands for kindly supplying the magnets used in this study. Ravi Kant Singh (chief consultant at Peace Pant Hospital, Varanasi, India) for providing the CT scans, Markus Steineck (University Center for Dental Medicine UZB, Basel, Switzerland) for supporting the magnet-based experiments and Hans Florian Zeilhofer for funding acquisition and support of the project.

Conflicts of Interest: The authors declare that they have no conflict of interest. The funders had no role in the design of the study; the collection, analysis, or interpretation of data; the writing of the manuscript; or the decision to publish the results.

References

1. Mossey, P. Global strategies to reduce the healthcare burden of craniofacial anomalies. *Br. Dent. J.* **2003**, *195*, 613. [[CrossRef](#)] [[PubMed](#)]
2. Mossey, P.A.; Little, J.; Munger, R.G.; Dixon, M.J.; Shaw, W.C. Cleft lip and palate. *Lancet* **2009**, *374*, 1773–1785. [[CrossRef](#)]
3. Schutte, B.C.; Murray, J.C. The many faces and factors of orofacial clefts. *Hum. Mol. Genet.* **1999**, *8*, 1853–1859. [[CrossRef](#)] [[PubMed](#)]
4. Mossey, P.A. Epidemiology of oral clefts: An international perspective. In *Cleft Lip and Palate: From Origin to Treatment*; Oxford University Press: Oxford, UK, 2002; ISBN 0195139062.
5. Mossey, P. Epidemiology underpinning research in the aetiology of orofacial clefts. *Orthod. Craniofac. Res.* **2007**, *10*, 114–120. [[CrossRef](#)]
6. Wong, F.K.; Hägg, U. An update on the aetiology of orofacial clefts. *Hong Kong Med. J.* **2004**, *10*, 331–336. [[PubMed](#)]
7. Nanci, A.; Ten, C.A.R. *Ten Cate's Oral Histology Development, Structure, and Function*; Elsevier: Amsterdam, The Netherlands, 2017.

8. Bush, J.O.; Jiang, R. Palatogenesis: Morphogenetic and molecular mechanisms of secondary palate development. *Development* **2012**, *139*, 231–243. [[CrossRef](#)]
9. Tarr, J.T.; Lambi, A.G.; Bradley, J.P.; Barbe, M.F.; Popoff, S.N. Development of normal and Cleft Palate: A central role for connective tissue growth factor (CTGF)/CCN2. *J. Dev. Biol.* **2018**, *6*, 18. [[CrossRef](#)]
10. Bühner, C.; Zimmermann, A. Cleft palate. In *Neonatal Emergencies: A Practical Guide for Resuscitation, Transport and Critical Care of Newborn Infants*; Cambridge University Press: Cambridge, UK, 2009; Volume 1, pp. 460–463. [[CrossRef](#)]
11. Huddart, A.G. Arch Alignment and Presurgical Treatment—The West Midlands Approach. In *Early Treatment of Cleft Lip and Palate*; Hans Huber: Berne, Switzerland, 1986; ISBN 3-456-81406-2.
12. Latief, B.S.; Lekkas, K.C.; Schols, J.G.J.H.; Fudalej, P.S.; Kuijpers, M.A.R. Width and elevation of the palatal shelves in unoperated unilateral and bilateral cleft lip and palate patients in the permanent dentition. *J. Anat.* **2012**, *220*, 263–270. [[CrossRef](#)]
13. Atherton, J.D. A Descriptive Anatomy of the Face in Human Fetuses with Unilateral Cleft Lip and Palate. *Cleft Palate J.* **1967**, *4*, 104–114. [[CrossRef](#)]
14. Diah, E.; Lo, L.J.; Huang, C.S.; Sudjatmiko, G.; Susanto, I.; Chen, Y.R. Maxillary growth of adult patients with unoperated cleft: Answers to the debates. *J. Plast. Reconstr. Aesthetic Surg.* **2007**, *60*, 407–413. [[CrossRef](#)]
15. Berkowitz, S.; Duncan, R.; Evans, C.; Friede, H.; Kuijpers-Jagtman, A.M.; Pahl-Anderson, B.; Rosenstein, S. Timing of Cleft Palate Closure Should Be Based on the Ratio of the Area of the Cleft to That of the Palatal Segments and Not on Age Alone. *Plast. Reconstr. Surg.* **2005**, *115*, 1483–1499. [[CrossRef](#)] [[PubMed](#)]
16. Kuijpers-Jagtman, A.M.; Long, R.E., Jr. The influence of surgery and orthopedic treatment on maxillofacial growth and maxillary arch development in patients treated for orofacial clefts. *Cleft Palate-Craniofac. J.* **2000**, *37*, 527. [[CrossRef](#)]
17. Nalabothu, P.; Benitez, B.K.; Dalstra, M.; Verna, C.; Mueller, A.A. Three-Dimensional Morphological Changes of the True Cleft under Passive Presurgical Orthopaedics in Unilateral Cleft Lip and Palate: A Retrospective Cohort Study. *J. Clin. Med.* **2020**, *9*, 962. [[CrossRef](#)] [[PubMed](#)]
18. McNeil, C.K. *Oral and Facial Deformity*; Pitman: London, UK, 1954.
19. Fish, J. Growth of the palatal shelves of post-alveolar cleft palate infants. Effects of stimulation appliances. *Br. Dent. J.* **1972**, *132*, 492–501. [[CrossRef](#)] [[PubMed](#)]
20. Huddart, A.G. Presurgical changes in unilateral cleft palate subjects. *Cleft Palate J.* **1979**, *16*, 147–157.
21. Pahl, C.; Kuijpers-Jagtman, A.M.; Van't Hof, M.A.; Pahl-Andersen, B. A randomised prospective clinical trial into the effect of infant orthopaedics on maxillary arch dimensions in unilateral cleft lip and palate (Dutchcleft). *Eur. J. Oral Sci.* **2001**, *109*, 297–305. [[CrossRef](#)]
22. Shaw, W.C.; Semb, G.; Nelson, P.; Brattström, V.; Mølsted, K.; Pahl-Andersen, B.; Gundlach, K.K.H. The Eurocleft project 1996–2000: Overview. *J. Cranio-Maxillofac. Surg.* **2001**, *29*, 131–140. [[CrossRef](#)]
23. Dorrance, G.M.; Shirazy, E. *The Operative Story of Cleft Palate*; W.B. Saunders Company: Philadelphia, PA, USA, 1933.
24. Campbell, B.Y.A. The closure of congenital clefts of the hard palate. *Br. J. Surg.* **1926**, *13*, 715–719. [[CrossRef](#)]
25. Pichler, H. Zur Operation der doppelten Lippen-Gaumenspalten. *Dtsch. Z. Cir.* **1926**, *195*, 104–107. [[CrossRef](#)]
26. Büttow, K.W. Caudally-based single-layer septum-vomer flap for cleft palate closure. *J. Cranio-Maxillofac. Surg.* **1987**, *15*, 10–13. [[CrossRef](#)]
27. Abyholm, F.E. Primary Closure of Cleft Lip and Palate. In *Facial Clefts and Craniosynostosis: Principles and Management*; Turvey, T.A., Vig, K.W.L., Fonseca, R.J., Eds.; W.B. Saunders Company: Philadelphia, PA, USA, 1996.
28. Langenbeck, B. Die Uranoplastik mittelst Ablösung des mucös-periostalen Gaumenüberzuges. Uranoplasty by means of raising mucoperiosteal flaps. Hirschwald: Berlin, 1861. *Plast. Reconstr. Surg.* **1972**, *49*, 326–330. [[CrossRef](#)]
29. Veau, V.; Borel, S. *Division palatine: Anatomie, Chirurgie Phonétique*/Victor Veau, Avec la Collaboration de S. Borel; Masson: Paris, France, 1931.
30. Bardach, J. Two-Flap palatoplasty: Bardach's technique. *Oper. Tech. Plast. Reconstr. Surg.* **1995**, *2*, 211–214. [[CrossRef](#)]
31. Millard, D.R., Jr. The island flap in cleft palate surgery. *Surg. Gynecol. Obstet.* **1963**, *116*, 297–300. [[CrossRef](#)]
32. Mukherji, M.M. Cheek flap for short palates. *Cleft Palate J.* **1969**, *6*, 415–420. [[PubMed](#)]

33. Stricker, M.; Chancholle, A.R.; Flot, F.; Malka, G.; Montoya, A. La greffe periostee dans la reparation de la fente totale du palais primaire [Periosteal graft in the repair of complete primary cleft palate]. *Ann. Chir. Plast.* **1977**, *22*, 117–125.
34. Neiva, C.; Dakpe, S.; Gbaguidi, C.; Testelin, S.; Devauchelle, B. Calvarial periosteal graft for second-stage cleft palate surgery: A preliminary report. *J. Cranio-Maxillofac. Surg.* **2014**, *42*, e117–e124. [\[CrossRef\]](#)
35. Shash, H.; Al-Halabi, B.; Jozaghi, Y.; Aldekhayel, S.; Gilardino, M.S. A review of tissue expansion-assisted techniques of cleft palate repair. *J. Craniofac. Surg.* **2016**, *27*, 760–766. [\[CrossRef\]](#) [\[PubMed\]](#)
36. Alkan, A.; Baş, B.; Özer, M.; Bayram, M. Closure of a large palatal fistula with maxillary segmental distraction osteogenesis in a cleft palate patient. *Cleft Palate-Craniofac. J.* **2007**, *44*, 112–115. [\[CrossRef\]](#)
37. Martín-Del-Campo, M.; Rosales-Ibañez, R.; Rojo, L. Biomaterials for cleft lip and palate regeneration. *Int. J. Mol. Sci.* **2019**, *20*, 2176. [\[CrossRef\]](#)
38. Schmidt, B.L.; Kung, L.; Jones, C.; Casap, N. Induced osteogenesis by periosteal distraction. *J. Oral Maxillofac. Surg.* **2002**, *60*, 1170–1175. [\[CrossRef\]](#)
39. Sencimen, M.; Aydıntug, Y.S.; Ortakoglu, K.; Karslioglu, Y.; Gunhan, O.; Gunaydin, Y. Histomorphometrical analysis of new bone obtained by distraction osteogenesis and osteogenesis by periosteal distraction in rabbits. *Int. J. Oral Maxillofac. Surg.* **2007**, *36*, 235–242. [\[CrossRef\]](#) [\[PubMed\]](#)
40. Sato, K.; Haruyama, N.; Shimizu, Y.; Hara, J.; Kawamura, H. Osteogenesis by gradually expanding the interface between bone surface and periosteum enhanced by bone marrow stem cell administration in rabbits. *Oral Surg. Oral Med. Oral Pathol. Oral Radiol. Endodontology* **2010**, *110*, 32–40. [\[CrossRef\]](#) [\[PubMed\]](#)
41. Darendeliler, M.A.; Darendeliler, A.; Mandurino, M. Clinical application of magnets in orthodontics and biological implications: A review. *Eur. J. Orthod.* **1997**, *19*, 431–442. [\[CrossRef\]](#)
42. Brand, R.A.; Stanford, C.M.; Swan, C.C. How do tissues respond and adapt to stresses around a prosthesis? A primer on finite element stress analysis for orthopaedic surgeons. *Iowa Orthop. J.* **2003**, *23*, 13–22.
43. Ghasemianpour, M.; Ehsani, S.; Tahmasbi, S.; Bayat, M.; Ghorbanpour, M.; Safavi, S.M.; Mirhashemi, F.S. Distraction osteogenesis for cleft palate closure: A finite element analysis. *Dent. Res. J.* **2014**, *11*, 92–99.
44. Nalabothu, P.; Verna, C.; Steineck, M.; Mueller, A.A.; Dalstra, M. The biomechanical evaluation of magnetic forces to drive osteogenesis in newborn's with cleft lip and palate. *J. Mater. Sci. Mater. Med.* **2020**, *31*, 1–8. [\[CrossRef\]](#)
45. Gundlach, K.K.H.; Maus, C. Epidemiological studies on the frequency of clefts in Europe and world-wide. *J. Cranio-Maxillofac. Surg.* **2006**, *34*, 1–2. [\[CrossRef\]](#)
46. Wang, D.; Cheng, L.; Wang, C.; Qian, Y.; Pan, X. Biomechanical analysis of rapid maxillary expansion in the UCLP patient. *Med. Eng. Phys.* **2009**, *31*, 409–417. [\[CrossRef\]](#)
47. McPherson, G.K.; Kriewall, T.J. The elastic modulus of fetal cranial bone: A first step towards an understanding of the biomechanics of fetal head molding. *J. Biomech.* **1980**, *13*, 9–16. [\[CrossRef\]](#)
48. Bauer, F.X.; Heinrich, V.; Grill, F.D.; Wölfl, F.; Hedderich, D.M.; Rau, A.; Wolff, K.D.; Ritschl, L.M.; Loeffelbein, D.J. Establishment of a finite element model of a neonate's skull to evaluate the stress pattern distribution resulting during nasoalveolar molding therapy of cleft lip and palate patients. *J. Cranio-Maxillofac. Surg.* **2018**, *46*, 660–667. [\[CrossRef\]](#)
49. Pan, X.; Qian, Y.; Yu, J.; Wang, D. Biomechanical Effects of Rapid Palatal Expansion on the Craniofacial Skeleton with cleft palate: A three-dimensional finite element analysis. *Cleft Palate-Craniofac. J.* **2007**, *44*, 149–154. [\[CrossRef\]](#) [\[PubMed\]](#)
50. Carter, D.R.; Schwab, G.H.; Spengler, D.M. Tensile fracture of cancellous bone. *Acta Orthop.* **1980**, *51*, 733–741. [\[CrossRef\]](#) [\[PubMed\]](#)
51. Kim, T.; Ishikawa, H.; Chu, S.; Handa, A.; Iida, J.; Yoshida, S. Constriction of the maxillary dental arch by mucoperiosteal denudation of the palate. *Cleft Palate-Craniofac. J.* **2002**, *39*, 425–431. [\[CrossRef\]](#) [\[PubMed\]](#)
52. Shetye, P.R.; Evans, C.A. Midfacial morphology in adult unoperated complete unilateral cleft lip and palate patients. *Angle Orthod.* **2006**, *76*, 810–816. [\[CrossRef\]](#)
53. Grayson, B.H.; Cutting, C.B. Presurgical nasoalveolar orthopedic molding in primary correction of the nose, lip, and alveolus of infants born with unilateral and bilateral clefts. *Cleft Palate-Craniofac. J.* **2001**, *38*, 193–198. [\[CrossRef\]](#)
54. Cutting, C.B.; Ortolani, A.; Bianchi, M.; Mosca, M.; Caravelli, S.; Fuiano, M.; Marcacci, M.; Russo, A. The prospective opportunities offered by magnetic scaffolds for bone tissue engineering: A review. *Joints* **2017**, *4*, 228–235. [\[CrossRef\]](#)

55. Ashley-Montagu, M.F. The form and dimensions of the palate in the newborn. *Int. J. Orthod. Dent. Child.* **1934**, *20*, 810–827. [[CrossRef](#)]
56. Frost, H.M. The Utah paradigm of skeletal physiology: An overview of its insights for bone, cartilage and collagenous tissue organs. *J. Bone Miner. Metab.* **2000**, *18*, 305–316. [[CrossRef](#)]
57. Stern, M.; Dodson, T.B.; Longaker, M.T.; Lorenz, H.P.; Harrison, M.R.; Kaban, L.B. Fetal cleft lip repair in lambs: Histologic characteristics of the healing wound. *Int. J. Oral Maxillofac. Surg.* **1993**, *22*, 371–374. [[CrossRef](#)]

Publisher’s Note: MDPI stays neutral with regard to jurisdictional claims in published maps and institutional affiliations.



© 2020 by the authors. Licensee MDPI, Basel, Switzerland. This article is an open access article distributed under the terms and conditions of the Creative Commons Attribution (CC BY) license (<http://creativecommons.org/licenses/by/4.0/>).